Fabrication and Analysis of β-Ga_2O_3 Schottky Diodes with Drift Layer Grown by MOCVD on (001) Substrate

Prakash P. Sundaram,[1] Fengdeng Liu,[1,2] Fikadu Alema,[3] Andrei Osinsky,[3] Bharat Jalan,[2] and Steven J. Koester[1]

[1] Dept. of Electrical and Computer Engineering, University of Minnesota, Minneapolis, MN 55455, USA
[2] Dept. of Chemical Engineering and Materials Science, University of Minnesota, Minneapolis, MN 55455, USA
[3] Agnitron Technology Incorporated, Chanhassen, MN 55317, USA
Tel: 1- 612-624-2285, Email: sunda098@umn.edu

Keywords: Gallium oxide, MOCVD, Schottky diode, ultra-wide bandgap.

Abstract

The growth of a thick, high-quality epitaxial layer on a β-Ga_2O_3 substrate is essential for the commercialization of β-Ga_2O_3 devices. Metal Organic Chemical Vapor Deposition (MOCVD) is a proven method for large-scale commercial growth and can also be used to produce high-quality β-$(AlGa)_2O_3$ heterostructures. This study focuses on the systematic examination of Schottky Barrier Diodes (SBDs) fabricated on two different Si-doped homoepitaxial β-Ga_2O_3 thin films grown on Sn-doped (001) and (010) β-Ga_2O_3 substrates using MOCVD. X-ray diffraction analysis, current density-voltage data at room temperature, and capacitance-voltage measurements are performed. The diode characteristics, such as the ideality factor, barrier height, and specific on-resistance, are also analyzed. The temperature dependence (from 170-360 K) of the ideality factor and barrier height is analyzed from the J-V-T characteristics of the fabricated Schottky diodes.

INTRODUCTION

β-Ga_2O_3 has gained significant attention as a promising ultra-wide bandgap (UWBG) semiconductor material for power electronics owing to its large bandgap of ~4.9 eV, high critical breakdown field of ~8 MV/cm and substantially large Baliga's figure of merit (BFOM) which is 4 (10) times greater than that of GaN (SiC).[1] The availability of affordable native single crystal substrates made from cost-effective melt-grown techniques, and the ability to grow high-quality epitaxial films with controllable doping, further make β-Ga_2O_3 attractive for high-power vertical devices.[2-4] Numerous studies been performed on the homoepitaxy of β-Ga_2O_3 on various substrate orientations using molecular beam epitaxy (MBE), metalorganic chemical vapor deposition (MOCVD), and halide vapor phase epitaxy (HVPE) growth methods.[5-7] Of all these techniques, MOCVD is the most well-established for large-scale commercial growth, and is used successfully for production of III-V and oxide-based power devices, LEDs and laser diodes, and is often employed for production of high-quality epitaxial wafers on an industrial scale.[8] MOCVD has the advantage of growing epitaxial films at a high growth rate of ~10 μm/hr with sub-nanometer surface roughness, without compromising film quality.[9] Compared to HVPE, MOCVD has a wider doping range, and can produce higher-quality β-$(AlGa)_2O_3$ thin films and heterostructures than HVPE.[10]

As far as the orientation of β-Ga_2O_3 is concerned, the principal planes, namely (100), (010), and (001) are often used for homoepitaxial thin-film growth. However, of these, only the (100) and (001) surface orientations of β-Ga_2O_3 are cleavage planes, making large diameter (> 6") wafer production possible.[11] Despite the advantage of these orientations, to date, growth of high-quality MOCVD films on (001) β-Ga_2O_3 has not been reported. Here, we demonstrate for the first time, the electrical characterization of Schottky barrier diode (SBD) fabricated on (001) β-Ga_2O_3 epi-layers grown by MOCVD.

GROWTH DETAILS AND X-RAY DIFFRACTION RESULTS

All epilayers were grown on Sn-doped β-Ga_2O_3 substrates in Agnitron's Agilis 500 MOCVD reactor using trimethylgallium (TMGa) and pure oxygen as precursors, N2 as carrier, and SiH_4 diluted in N_2 for Si doping. To compare and evaluate the characteristics of the films grown on (001)-oriented substrates, epilayers were also co-grown on Fe dopped (010) β-Ga_2O_3 substrates. The films were grown at a pressure of 15 Torr and a substrate temperature of 825 °C. The growth rate for the (001) epilayer was ~0.62 μm/hr, while the (010) epilayer has a growth rate of 0.75 μm/hr. The thickness of (001) and (010) epilayers were found to be 3.3 μm and 3.5 μm, respectively. A target doping concentration of ~1×10^{16} cm^{-3} was used for each sample as determined by Hall effect measurements on a witness sample grown on (010) Fe-doped β-Ga_2O_3 substrates, which were co-loaded with the Sn-doped substrates.

The crystal quality of the (001) epilayer was analyzed by x-ray diffraction (XRD) rocking curve and 2θ-ω measurements using a Cu Kα source (λ = 1.54 Å). The diffraction patterns (Fig. 1) of the film include sharp (001), (002), (003) and (004) diffraction peaks, indicating pure β-Ga_2O_3 and a single preferred growth orientation along the <001> direction. The absence of any peaks related to α, γ, δ, and ε phases of Ga_2O_3 suggests that the thin film is composed of single-phase β-Ga_2O_3 on the (001) substrate. The full width at half maximum (FWHMs) from rocking curve measurements (Fig. 1 inset) for the (001) sample is 0.34°. This value is higher than that of the substrate, a fact that can be attributed to mosaic twist distribution in the epilayer.[12]

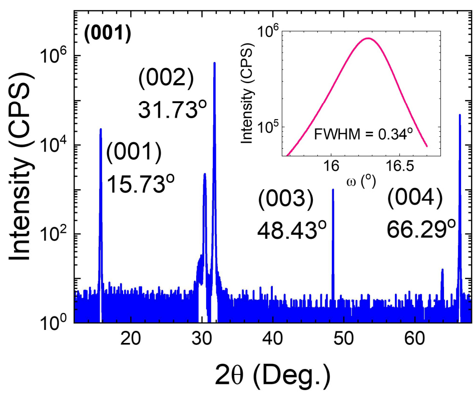

Fig 1. X-ray diffraction (XRD) 2θ-ω profile of the sample of MOCVD grown (001) film on (001) substrate. The inset shows the ω rocking curve of (002) plane.

The FWHM for the (010) epilayer, grown under similar conditions, was reported to be lesser than 0.011° by Agnitron in previous studies and this level of quality is comparable to that of bulk substrates.[13]

DEVICE FABRICATION AND EXPERIMENTAL RESULTS

SBDs were fabricated on both the (010) and (001) epilayers to verify and compare their electrical properties.

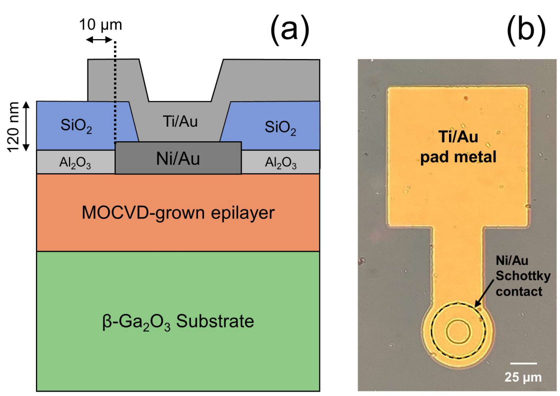

Fig. 2. (a) Cross-sectional view of SBD fabricated on MOCVD-grown epilayer on (001) and (010) samples and (b) an optical micrograph of a fabricated SBD with 50 μm diameter.

The device fabrication process commenced with BCl_3-based reactive-ion etching (RIE) of the backside, while the front side was protected with photoresist. A total of 1 μm thick β-Ga_2O_3 was etched in this step. Next, a blanket Ti (30 nm) / Au (125 nm) Ohmic metal stack was deposited by electron-beam evaporation onto the backside. In order to protect the sample surface from potential O_2 plasma damage in subsequent lithographic steps, a 20-nm-think Al_2O_3 sacrificial layer was first deposited on the epilayer by atomic layer deposition (ALD) at 200 °C. The samples were then patterned using standard photolithography, and circular active regions with a diameter ranging from 30 to 100 μm were opened. After removing the Al_2O_3 sacrificial layer using a wet etch, a Ni/ (30 nm) / Au (50 nm) Schottky metal stack of thickness was deposited by electron-beam evaporation, followed by a lift-off process. Initially, reverse-biased room-temperature capacitance-voltage (C-V) measurements were performed on the Schottky contacts using Agilent B1500A semiconductor parameter analyzer in order to extract the epilayer doping concentration, N_D.

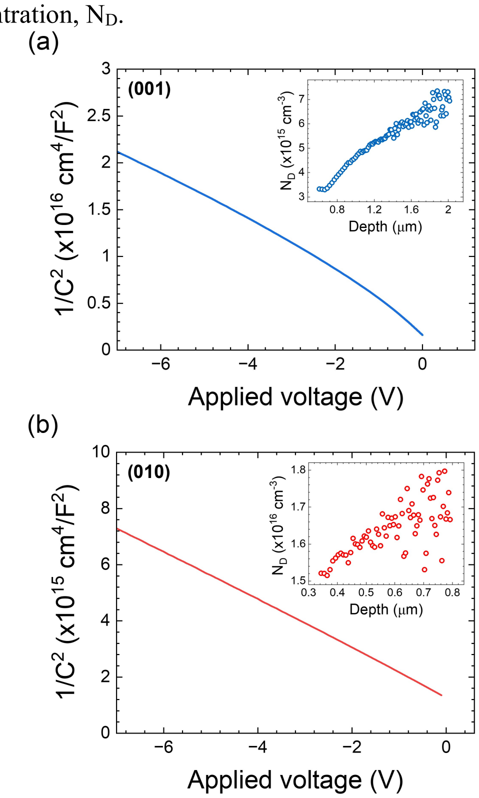

Fig. 3. C-V characteristics measured at room temperature at 100 kHz of SBDs with 300 μm diameter from the (a) (001) and (b) (010) oriented sample. The insets show the extracted net doping concentration from C-V measurements.

Fig. 3 shows an N_D in the range of 0.3 - 0.7 × 10^{16} cm^{-3} for the (001) samples which is slightly lower than the expected doping from the (010) witness and control samples, indicating there are possibly inactive dopants in the (001) epilayer and additional optimization of growth process might be needed. Next, current-voltage measurements were performed to measure the Schottky barrier height (SBH) of the Ni contacts to both the (001) and (010) samples. All devices were measured at room temperature in air. The measurements were carried out with the cathode grounded and the anode bias voltage swept from 0 to 1.5 V in 30 mV steps. The maximum current density was limited to about 25 A/cm^2 for all devices to avoid damaging the devices. Figs. 3(a) and 3(b) show the forward current density versus voltage (J-V) characteristics of typical SBDs on the (001) and (010) samples, respectively. In order to estimate the ideality factor and Schottky barrier height of the Ni-semiconductor interface, the J-V data was fit using thermionic emission (TE) equation. As shown in Fig. 4, for J up to 10 mA/cm^2, the TE model fits well for both the (001) and (010) SBDs. The value of Φ_B can be determined by fitting TE model in the linear region of the log(J) vs. V characteristics, and the extracted SBHs were $\Phi_B = 1.08 \pm 0.02$ eV and 1.25 ± 0.02 eV for the (001) and (010) devices, respectively.

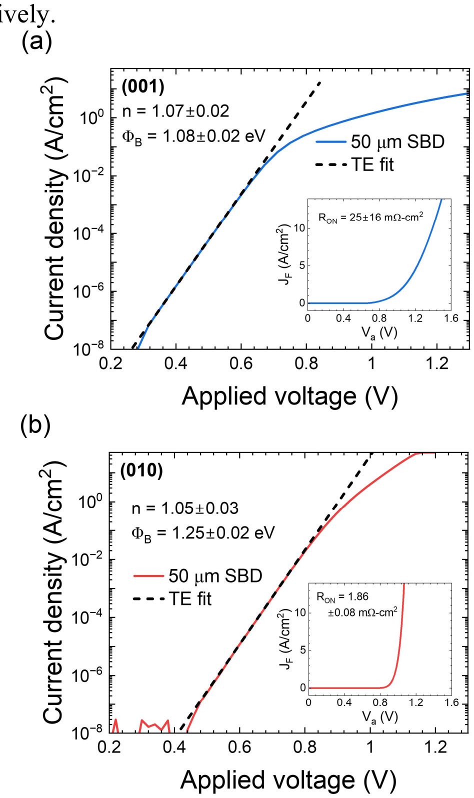

Fig. 4. Room-temperature experimental forward J-V characteristics of SBDs with thermionic emission (TE) model fitting parameters, n and Φ_B of the (a) (001) and (b) (010) oriented sample. The insets show the same J-V plots on a linear scale.

This result is consistent with literature results for HVPE-grown layers on (001) substrates.[14] The (001) sample shows an on-state resistance, R_{ON} of 25 ± 16 mΩ-cm^2 (Fig. 4) which is over 10 times that of the (010) control sample. While the higher resistance is partially due to 3-4x lower doping in the (001) samples, other factors such as lower mobility and interfacial issues at the growth interface could also be contributing factors. Further studies such as Hall measurements and transmission line measurement test structures are necessary to fully understand the higher R_{ON}. A value of $n = 1.07 \pm 0.02$ was extracted for the (001) samples from the exponential region of the forward J-V characteristics for the (001) samples, and this value is similar to that obtained for the (010) samples. The temperature-dependent forward J-V characteristics of SBDs of (001) and (010) samples are shown in Fig. 5. The current density for the given applied voltage increases monotonically as the temperature increases as modelled by the thermionic emission equation.

The Φ_B and n for both samples are plotted vs. T in Fig. 6. Φ_B (n) is seen to increase (decrease) monotonically with increasing temperature. Such temperature-dependent behavior is consistent with barrier height inhomogeneity at the Schottky interface.[15] Among the several reasons for SBH inhomogeneity that have been reported in the literature, a likely reason is that the interface is not atomically flat throughout the metal-semiconductor contact due to surface roughness. Other possibilities could include surface and bulk defects, surface treatments, vacancy-related defects, and dislocations, all of which can produce local variation of electric field at the metal-semiconductor interface.

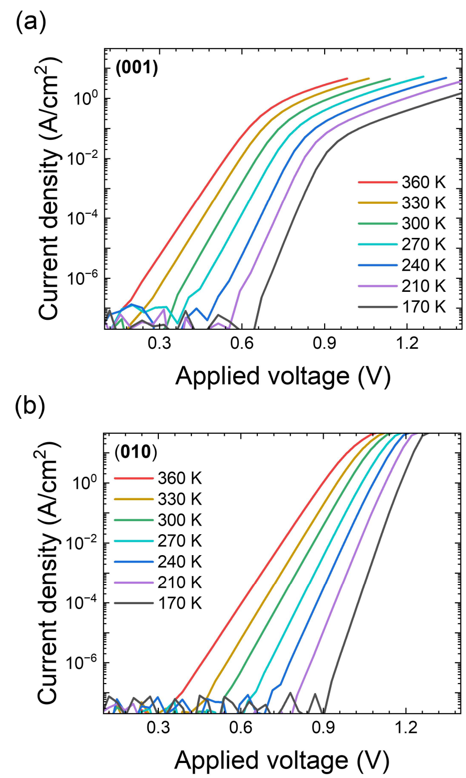

Fig. 5. Temperature-dependent forward J-V characteristics of an SBD on the (a) (001) and (b) (010) oriented sample, with a temperature range between 170 K and 360 K.

The TE model assumes an atomically flat and homogeneous metal-semiconductor interface, but an inhomogeneous surface interface consists of locally non-uniform regions having lower and higher barrier height patches at the nanoscale. At lower temperatures, current conduction is due to carriers which cross the patches having relatively lower barrier heights, while at higher temperatures current conduction is dominated by those carriers which cross the patches having relatively higher barrier heights. Such temperature-dependent anomalies in SBH and n can be modeled by assuming a Gaussian distribution of apparent barrier height, Φ_{ap}, measured experimentally with mean barrier height, $\overline{(\Phi_{b0})}$, standard deviation, σ_s, and apparent ideality factor, n_{ap}, from experimental data, using analytical potential fluctuation model proposed by Werner and Gutter.[16]

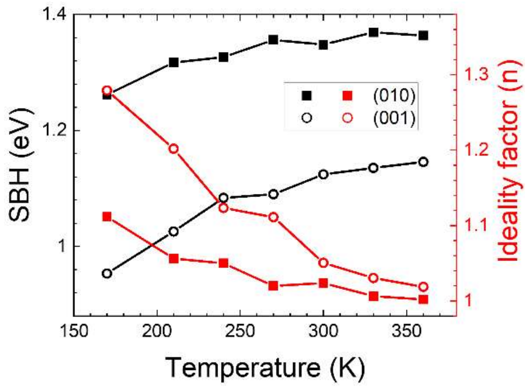

Fig. 6. Extracted Φ_B (black) and n (red) using a thermionic model from temperature-dependent forward J-V characteristics of SBDs from both (001) and (010) oriented samples.

From the Fig. 6, it can be seen that the temperature-dependence of Φ_B is slightly more pronounced for the (001) sample than for (010), indicating the former has relatively higher SBH inhomogeneity. As far as reverse breakdown measurement is concerned, additional metallization on the SBDs is needed and these results will be reported at a later time.

CONCLUSIONS

We have presented the physical and electrical characteristics of MOCVD-grown (001) β-Ga_2O_3 SBDs and compared the results with those grown on (010) epi-layers. The (001)-grown samples show lower SBH for Ni contacts than those on (010) substrates. The temperature-dependence of the barrier height obtained from fitting the forward J-V characteristics indicate the presence of barrier height inhomogeneity for both samples, but more prominently in the (001) samples. Due to the numerous advantages of MOCVD and (001)-orientation substrates, this is a significant milestone in development and commercialization of β-Ga_2O_3 devices for power applications.

ACKNOWLEDGEMENTS

P.P.S. and S.J.K. acknowledge support by the University of Minnesota Futures grant program and the Air Force Office of Scientific Research (AFOSR) under award number FA9550-19-1-0245. F.A. and A.O acknowledge the Office of Naval Research under award number N6833518C0192. Portions of this work were conducted in the Minnesota Nano Center, which is supported by the National Science Foundation (NSF) through the National Nanotechnology Coordinated Infrastructure (NNCI) under award number ECCS-2025124. Parts of this work were carried out in the Characterization Facility, University of Minnesota, which receives partial support from the NSF through the MRSEC programs (Award Number DMR-2011401).

[1] M. Higashiwaki and G. H. Jessen, Appl. Phys. Lett. 112, 060401 (2018).

[2] M. Higashiwaki, K. Sasaki, A. Kuramata, T. Masui, and S. Yamakoshi, Phys. Status Solidi A 211, 21-26 (2014).

[3] H. Murakami, K. Nomura, K. Goto, K. Sasaki, K. Kawara, Q. T. Thieu, R. Togashi, Y. Kumagai, M. Higashiwaki, A. Kuramata, S. Yamakoshi, B. Monemar, and A. Koukitu, Appl. Phys. Express, 8, 015503 (2015).

[4] K. Sasaki, A. Kuramata, T. Masui, E. G. Villora, K. Shimamura, and S. Yamakoshi, Appl. Phys. Express 5, 035502 (2012).

[5] N. K. Kalarickal, Z. Xia, J. McGlone, S. Krishnamoorthy, W. Moore, M. Brenner, A. R. Arehart, S. A. Ringel, and S. Rajan, Appl. Phys. Lett. 115, 152106 (2019).

[6] J. H. Leach, K. Udwary, J. Rumsey, G. Dodson, H. Splawn, and K. R. Evans, APL Materials 7, 022504 (2019).

[7] Y. Zhang, F. Alema, A. Mauze, O. S. Koksaldi, R. Miller, A. Osinsky, and J. S. Speck, APL Materials 7, 022506 (2019).

[8] M. J. Tadjer, M. A. Mastro, N. A. Mahadik, M. Currie, V. D. Wheeler, J. A. Freitas, J. D. Greenlee, J. K. Hite, K. D. Hobart, C. R. Eddy, and F. J. Kub, J. Electron. Mater. 45, 2031 (2016).

[9] F. Alema, B. Hertog, A. Osinsky, P. Mukhopadhyay, M. Toporkov, and W. V. Schoenfeld, Journal of Crystal Growth 475, 77-82 (2017).

[10] M. Higashiwaki, and S. Fujita, Springer Series in Materials Science; Springer International Publishing: Cham, Switzerland, 2020; Volume 293, ISBN 9783030371524.

[11] V.M. Bermudez, Chem. Phys. 323, 193-203 (2006).

[12] S. Saha, L. Meng, Z. Feng, A. F. M. A. U. Bhuiyan, H. Zhao, and U. Singisetti, Appl. Phys. Lett. 120, 122106 (2022).

[13] F. Alema, Y. Zhang, A. Osinsky, N. Orishchin, N. Valente, A. Mauze, and J. S. Speck, APL Materials 8, 021110 (2020).

[14] J. Yang, S. Ahn, F. Ren, S. J. Pearton, S. Jang, J. Kim, and A. Kuramata, Appl. Phys. Lett. 110, 192101 (2017).

[15] J. H. Werner, and H. H. Guttler, Journal of Applied Physics 69, 1522-1533 (1991).

[16] J. H. Werner, and H. H. Guttler, Journal of Applied Physics 69, 1522-1533 (1991).